Cell Reports

Report

Single-Stranded DNA-Binding Transcriptional Regulator FUBP1 Is Essential for Fetal and Adult Hematopoietic Stem Cell Self-Renewal

Graphical Abstract

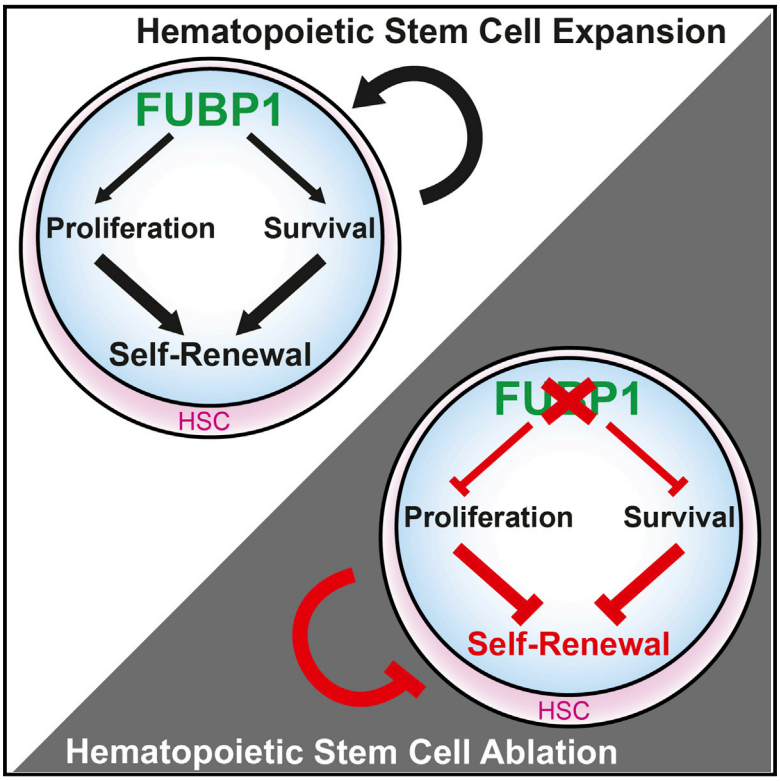

Highlights

- FUBP1 is required for the expansion of LT-HSCs in the fetal liver
- FUBP1 is essential for fetal and adult LT-HSC self-renewal
- Loss of FUBP1 results in increased LT-HSC cell death and prolonged cell cycle
- Loss of FUBP1 does not prevent the differentiation into all hematopoietic lineages

Authors

Uta Rabenhorst, Frederic B. Thalheimer, Katharina Gerlach, ..., Harald von Melchner, Michael A. Rieger, Martin Zörnig

Correspondence

m.rieger@em.uni-frankfurt.de (M.A.R.), zoernig@gsh.uni-frankfurt.de (M.Z.)

In Brief

Self-renewal of hematopoietic stem cells (HSCs) is required for definitive fetal and adult hematopoiesis. Rabenhorst et al. demonstrate an essential function of the single-stranded DNA-binding transcriptional regulator *FUSE*-binding protein 1 (FUBP1) for the expansion and maintenance of HSCs by modulating HSC proliferation and survival.

Rabenhorst et al., 2015, Cell Reports *11*, 1847–1855
June 30, 2015 ©2015 The Authors
http://dx.doi.org/10.1016/j.celrep.2015.05.038

CellPress

Cell Reports
Report

OPEN ACCESS
CellPress

Single-Stranded DNA-Binding Transcriptional Regulator FUBP1 Is Essential for Fetal and Adult Hematopoietic Stem Cell Self-Renewal

Uta Rabenhorst,[1,7,9] Frederic B. Thalheimer,[2,7] Katharina Gerlach,[1,7] Marek Kijonka,[1] Stefanie Böhm,[1,10] Daniela S. Krause,[1] Franz Vauti,[3] Hans-Henning Arnold,[3] Timm Schroeder,[4] Frank Schnütgen,[2] Harald von Melchner,[2] Michael A. Rieger,[2,5,6,8,*] and Martin Zörnig[1,8,*]

[1]Georg-Speyer-Haus, Institute for Tumor Biology and Experimental Therapy, 60596 Frankfurt am Main, Germany
[2]LOEWE Center for Cell and Gene Therapy Frankfurt and Department for Hematology/Oncology, Goethe University Hospital Frankfurt, 60590 Frankfurt am Main, Germany
[3]Department of Cellular and Molecular Neurobiology, Technical University of Braunschweig, Spielmannstrasse 7, 38106 Braunschweig, Germany
[4]Department of Biosystems Science and Engineering (D-BSSE), ETH Zurich, Mattenstrasse 26, 4058 Basel, Switzerland
[5]German Cancer Consortium (DKTK), 69120 Heidelberg, Germany
[6]German Cancer Research Center (DKFZ), Im Neuenheimer Feld 280, 69120 Heidelberg, Germany
[7]Co-first author
[8]Co-senior author
[9]Present address: Department of Biosciences and Nutrition, NOVUM, Karolinska Institute, 141 83 Huddinge, Sweden
[10]Present address: Department of Microbiology and Molecular Genetics, University of Pittsburgh School of Medicine, University of Pittsburgh Cancer Institute, Pittsburgh, PA 15213, USA
*Correspondence: m.rieger@em.uni-frankfurt.de (M.A.R.), zoernig@gsh.uni-frankfurt.de (M.Z.)
http://dx.doi.org/10.1016/j.celrep.2015.05.038
This is an open access article under the CC BY-NC-ND license (http://creativecommons.org/licenses/by-nc-nd/4.0/).

SUMMARY

The ability of hematopoietic stem cells (HSCs) to self-renew is a prerequisite for the establishment of definitive hematopoiesis and life-long blood regeneration. Here, we report the single-stranded DNA-binding transcriptional regulator far upstream element (*FUSE*)-binding protein 1 (FUBP1) as an essential factor of HSC self-renewal. Functional inactivation of FUBP1 in two different mouse models resulted in embryonic lethal anemia at around E15.5 caused by severely diminished HSCs. Fetal and adult HSCs lacking FUBP1 revealed an HSC-intrinsic defect in their maintenance, expansion, and long-term blood reconstitution, but could differentiate into all hematopoietic lineages. FUBP1-deficient adult HSCs exhibit significant transcriptional changes, including upregulation of the cell-cycle inhibitor *p21* and the pro-apoptotic *Noxa* molecule. These changes caused an increase in generation time and death of HSCs as determined by video-microscopy-based tracking. Our data establish FUBP1 and its recognition of single-stranded genomic DNA as an important element in the transcriptional regulation of HSC self-renewal.

INTRODUCTION

Long-term repopulating hematopoietic stem cells (LT-HSCs) give rise to the lifelong regeneration of all mature blood cell lineages. They are at the apex of the hematopoietic differentiation hierarchy consisting of several progenitor cell stages with restricted stemness and lineage potential (Orkin and Zon, 2008; Rieger and Schroeder, 2012). During embryonic development, definitive LT-HSCs colonize the fetal liver (FL) and expand extensively by undergoing rapid self-renewal divisions to establish the pool of LT-HSCs required for adult life. In contrast, adult LT-HSCs primarily reside in a quiescent G_0 cell-cycle phase, rarely divide, and are maintained at constant cell numbers (Pietras et al., 2011; Qiu et al., 2014; Wilson et al., 2008) to ensure lifelong blood regeneration. LT-HSC self-renewal is significantly increased only during hematopoietic stress conditions, such as infections, anemia, or bone marrow (BM) cell depletion, e.g., upon chemotherapeutic treatment (Wilson et al., 2008).

Although transcription factors essential for the establishment of definitive LT-HSCs in fetal tissues have been identified, such as RUNX1 (Samokhvalov et al., 2007) and TAL1 (Mikkola et al., 2003; Schlaeger et al., 2005), the transcriptional network that governs the self-renewal and expansion programs in LT-HSCs remains poorly understood. Furthermore, identification of the essential components of the self-renewal program is key to achieving a robust expansion of LT-HSCs ex vivo (Nishino et al., 2012; Wohrer et al., 2014).

We have previously identified FUBP1 as an anti-apoptotic and pro-proliferative oncoprotein that is overexpressed in hepatocellular carcinomas (HCCs) (Malz et al., 2009; Rabenhorst et al., 2009). FUBP1 functions as a transcriptional regulator by binding to the single-stranded DNA element *FUSE* and interacting with the basal transcriptional machinery (Chung and Levens, 2005). Target genes regulated by FUBP1 include the

immediate early gene *c-myc* (Duncan et al., 1994), the cell-cycle inhibitor *p21* (Rabenhorst et al., 2009), and the deubiquitinating enzyme *Usp29* (Liu et al., 2011). To study the physiological function of FUBP1 in vivo, we generated gene trap mouse models lacking FUBP1 activity. The homozygous *Fubp1*$^{null/null}$ gene trap embryos die in utero at approximately day E15.5 with a severe anemic phenotype, thereby indicating that FUBP1 plays a role in hematopoietic development and/or homeostasis.

Our analyses demonstrate that FUBP1 is specifically required for LT-HSC self-renewal and survival during fetal and adult hematopoiesis, while its absence does not prevent the generation of all hematopoietic cell lineages. The operating mode of FUBP1 suggests that the presence of single-stranded genomic DNA structures represents an additional level of self-renewal regulation.

RESULTS AND DISCUSSION

FUBP1 Inactivation Results in Embryonic Lethality and Loss of LT-HSCs

Motivated by our previous studies on the oncogenic function of *FUBP1*, we generated two independent gene trap mouse lines (GT 1 and GT 2) that lack WT FUBP1 protein (Figure 1B; for further details, see Experimental Procedures). Both strains exhibited a similar phenotype. Accordingly, all homozygous mice derived from heterozygous matings died at approximately day E15.5 and were severely anemic (Figure 1A). The total FL cell numbers in E15.5 *Fubp1*$^{null/null}$ embryos were markedly reduced (Figure 1C). However, the proportion and subtype distribution of the colony-forming progenitor cells (CFU-GM, CFU-GEMM, and CFU-MK-E) were similar in the WT and FUBP1-deficient FLs (Figure 1D). When we analyzed the hematopoietic stem and progenitor cell (HSPC) populations by their well-established surface marker profile (Figures 1E and 1F; Table S1) (Kim et al., 2006), we found that fetal LT-HSCs (CD150^{+} CD48^{-} Mac-1^{+} KSL) were severely reduced in proportion and number in the FUBP1-deficient FLs (Figure 1F, left). In contrast, the numbers of CD150^{-} CD48^{+} MPPs and Mac-1^{+} KSL (immature compartment; Morrison et al., 1995) cells remained largely unaffected by the absence of FUBP1 (Figure 1F, middle and right). To test whether the anemia observed in homozygous mutant *Fubp1*$^{null/null}$ embryos is mainly caused by the loss of definitive LT-HSCs, we analyzed the different erythroid progenitors and myelocytes in peripheral blood (PB) and FL of WT and FUBP1-deficient embryos at E11.5, when the majority of red blood cells still originate from the HSC-independent primitive lineages. Our data showed that erythropoiesis and myelopoiesis at this early stage appear unaffected by the absence of FUBP1 (Figures S1A and S1B).

The analysis of colony-forming cells (Figure 1D), MPPs, and Mac-1^{+} KSL cells (Figure 1F) indicated that FUBP1, while essential for the maintenance of LT-HSCs, might be dispensable for the differentiation of the different hematopoietic lineages. To confirm this conclusion, we analyzed the proportion of hematopoietic lineages in the FL of E15.5 embryos. As shown in Figure S1C, the myelomonocytic, erythroid, and lymphocytic lineages (B and T cells) are present in equal proportions in WT and *Fubp1*$^{null/null}$ FL.

We then prospectively isolated MEPs, GMPs, LMPPs, and MPP2s from E15.5 FL (gating strategy shown in Figure S2A) and evaluated their colony-formation potential. Equal numbers and comparable types of colonies with similar size were generated from all WT and *Fubp1*$^{null/null}$ progenitor cell populations (Figures S2B and S2C), supporting the notion that all hematopoietic lineages are generated in the absence of FUBP1.

Fetal LT-HSCs Require FUBP1 for Self-Renewal and Long-Term Repopulation

To functionally validate the cell surface marker-based analyses that indicated lack of *Fubp1*$^{null/null}$ LT-HSCs in FLs at E15.5, we competitively transplanted 5 × 10^{4} lin^{-} WT or *Fubp1*$^{null/null}$ (GT 1) FL cells into lethally irradiated recipient mice (Figure 2A) and monitored donor cell repopulation in the PB. Consistent with the anemic phenotype of FUBP1-deficient embryos, *Fubp1*$^{null/null}$ FL cell engraftment was significantly reduced when compared with the WT FL cell engraftment (Figure 2B). Importantly, no major differences in the contribution of B, T, and myeloid cells from WT or *Fubp1*$^{null/null}$ donor cells were observed (Figure 2C), further supporting the notion that FUBP1 is dispensable for multilineage differentiation.

Then, we investigated the HSPC composition in primary recipient BM at 11 and 21 weeks to evaluate whether the reduced primary engraftment was due to a reduction or complete depletion of the HSC population. While the proportion of donor-derived MPPs was similar between recipients receiving *Fubp1*$^{null/null}$ or WT cells, the percentage of FUBP1-deficient LT-HSCs had already decreased 11 weeks after transplantation (Figures 2D and 2E), and virtually no *Fubp1*$^{null/null}$ LT-HSCs were detected after 21 weeks (original flow cytometry plots and gating strategies for the BM analyses are displayed in Figure S3).

To validate the absence of phenotypic FUBP1-deficient LT-HSCs after 21 weeks in primary recipient BM, displaying inability to self-renew, we serially transplanted 1 × 10^{4} WT or *Fubp1*$^{null/null}$ CD45.2^{+} lin^{-} c-Kit^{+} BM cells (BMCs) competitively into lethally irradiated recipient mice (Figure 2A). Flow cytometry analysis of PB and BM revealed no engraftment of *Fubp1*$^{null/null}$ donor cells due to the complete absence of LT-HSCs (Figures 2F and 2G), whereas WT donor cells long-term engrafted. The transplantation data clearly confirmed the low number of definitive LT-HSCs in *Fubp1*$^{null/null}$ FLs at E15.5 with impaired self-renewal capacity.

Collectively, our results demonstrate that functional FUBP1 is required for definitive LT-HSC self-renewal, expansion, and long-term repopulation capacity in the FL.

FUBP1 Is Essential for Adult HSC Self-Renewal

Given that we observed that FUBP1-deficient mice lack phenotypic and functional LT-HSCs in the FL, we hypothesized that LT-HSCs intrinsically require FUBP1 for self-renewal and expansion during definitive hematopoiesis. To verify this hypothesis and assess the functional consequences of FUBP1 deficiency on LT-HSC fate decisions, we knocked down *Fubp1* in adult murine LT-HSCs using two different lentiviral shRNA constructs. Next, we competitively transplanted adult LT-HSCs that were lentivirally transduced with shRNAs against *Fubp1* or a *scrambled* control into lethally irradiated recipient mice (Figure 3A). Expression

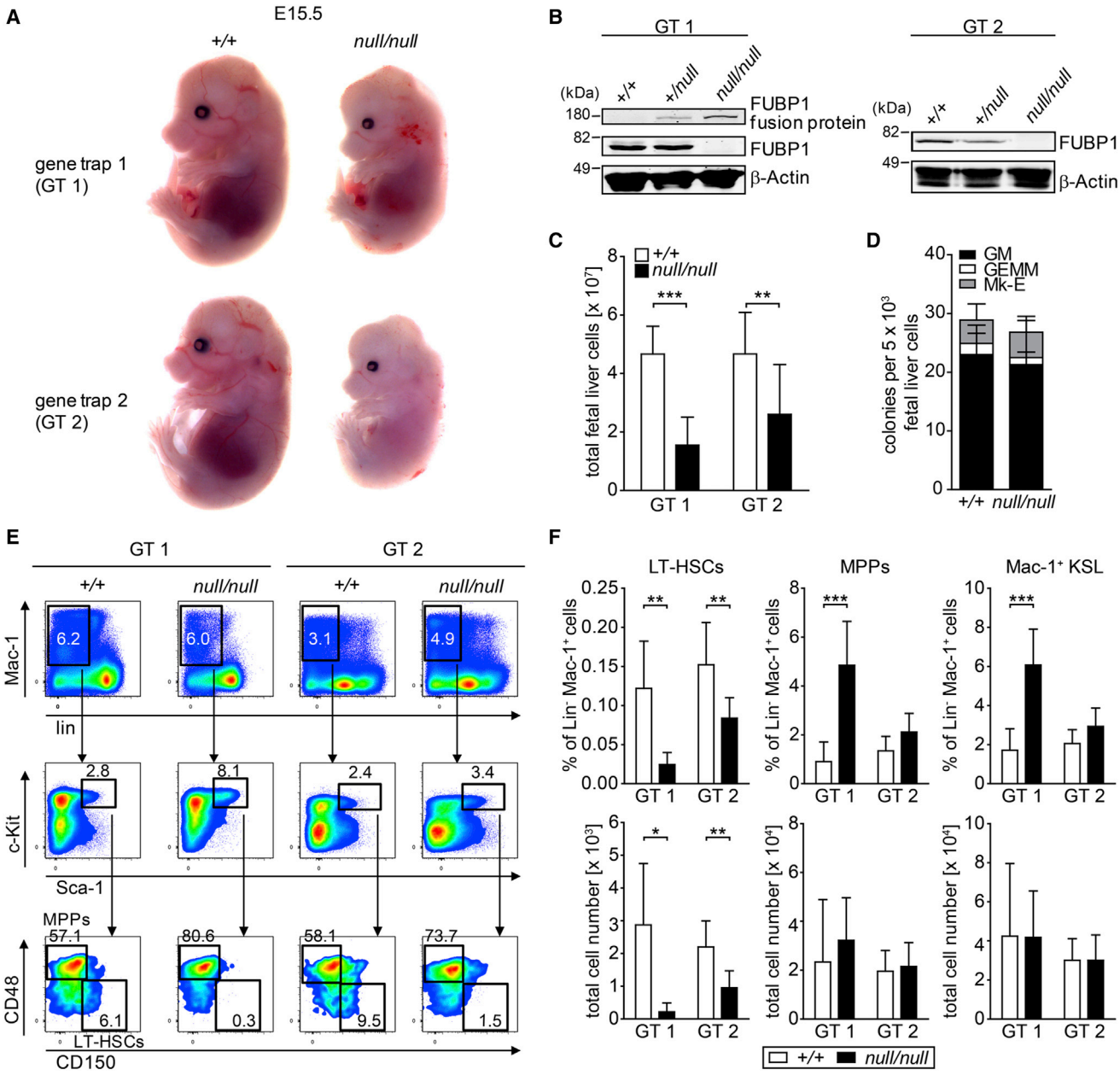

Figure 1. Loss of Murine FUBP1 Activity Resulted in Embryonic Lethality and a Reduction in LT-HSCs

(A) *Fubp1*$^{null/null}$ embryos of both gene trap (GT) models displayed a severe anemic phenotype and died at approximately day E15.5.

(B) Western blot analysis demonstrated the complete loss of WT FUBP1 protein expression in homozygous *Fubp1*$^{null/null}$ gene trap mice. Protein lysates were isolated from E13.5 MEFs (GT 1) and E15.5 embryos (GT 2).

(C) FL total cell number (+/+: n = 18 [GT 1], n = 17 [GT 2], *null/null*: n = 12 [GT 1], n = 12 [GT 2]; seven and four independent experiments for GT 1 and GT 2, respectively; unpaired t test).

(D) Colony-formation potential of GT 1 E15.5 FL cells (+/+: n = 5, *null/null*: n = 5; two independent experiments).

(E and F) HSPCs in *Fubp1*$^{null/null}$ and WT E15.5 FLs determined via flow cytometry. (E) Representative flow cytometry plots. (F) Relative and absolute flow cytometric quantification (WT: n = 6 [GT 1], n = 6 [GT 2], *null/null*: n = 5 [GT 1], n = 8 [GT 2]; two independent experiments). Test for statistical significance: unpaired Student's t test. Data are represented as the mean and SD.

of both *Fubp1* shRNAs led to a significant reduction in the amount of FUBP1 protein. Of note, shRNA #2 was more efficient in reducing FUBP1 levels (Figure 3B). Knockdown of *Fubp1* in LT-HSCs drastically reduced blood cell reconstitution in the PB and BM over time (Figures 3C and 3E). However, similar to the FUBP1-deficient FL cells, the knockdown of *Fubp1* in LT-HSCs did not prevent the generation of all hematopoietic lineages (Figure 3D).

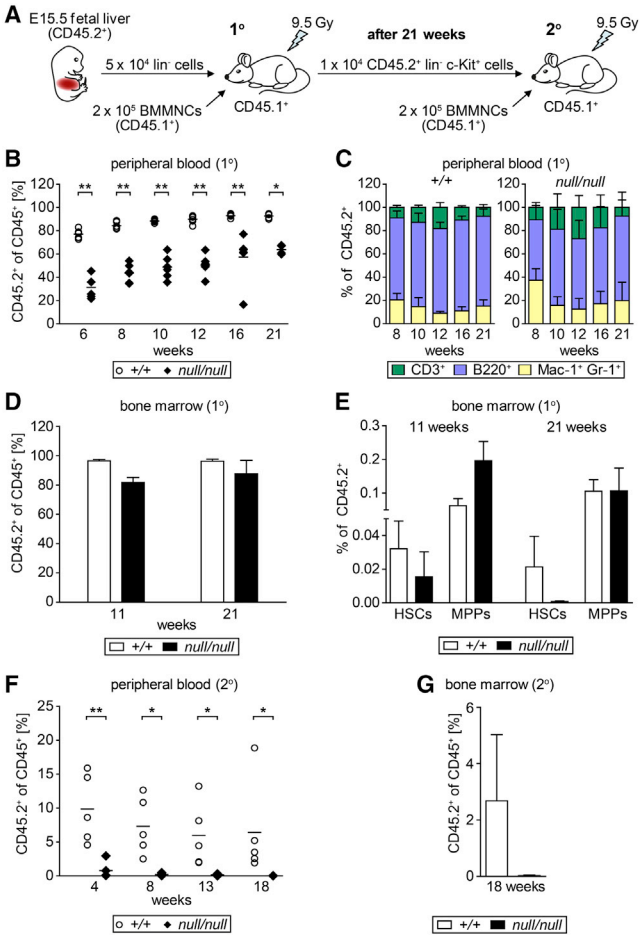

Figure 2. FUBP1-Deficient FLs Contain Less Functional LT-HSCs with Diminished Self-Renewal Capacity

(A) Experimental scheme.

(B–E) Multi-lineage donor cell reconstitution ($CD45.2^+$) of lethally irradiated recipient mice (seven per group; one experiment) after competitive transplantation of FUBP1-deficient E15.5 FL cells (GT 1) compared with WT cells, measured in PB (B and C) and BM (D and E) by flow cytometry (n = 3 mice for D and E).

(F and G) *Fubp1*$^{null/null}$ $CD45.2^+$ lin^- c-Kit^+ cells isolated from the BM of primary recipients failed to engraft upon secondary transplantation in PB (F, n = 5) and BM (G, n = 3). Test for statistical significance: Mann-Whitney; bar charts represent the mean and SD.

To establish whether adult LT-HSCs require FUBP1 for self-renewal, we performed secondary transplantations of equal numbers of transduced ($CD45.2^+$ $Venus^+$) cells isolated from the BM 8 weeks after the primary transplant (Figure 3A). The PB analysis from week 2 to week 18 post-secondary transplantation (Figure 3F) and the terminal analysis of the BM at 20 weeks (Figure 3H) showed markedly reduced blood cell reconstitution of the *Fubp1* knockdown donor cells compared with the control donor cells (*scrambled* shRNA). From week 14 on after transplantation, *Fubp1* knockdown donor cells contributed less than 1% to the total number of $CD45^+$ cells in PB, while scrambled control shRNA-transduced donor cells remained stable above 1% contribution (Figure 3F). In the BM, the difference is even more obvious, with more than 10% of scrambled control donor cells contributing to the total number of $CD45^+$ cells, while FUBP1-deficient cells again provided less than 1% of all $CD45^+$ cells (Figure 3H). These data demonstrate the absence of LT-HSCs in primary recipient BM after *Fubp1* knockdown. Intriguingly, multilineage differentiation was not affected (Figure 3G). Of note, LT-HSCs transduced with *Fubp1* shRNA #1, which displayed less knockdown efficiency, showed a slightly higher chimerism than *Fubp1* shRNA #2-transduced LT-HSCs in both the primary and secondary transplantations.

Because the amount of transduced *Fubp1* knockdown donor cells was already low 8 weeks after primary transplantation, we were limited to a small number of recipient mice in our secondary transplantation experiments. Consequently, the injection of the same small number of *scrambled* shRNA-transduced donor cells resulted in a rather low engraftment. Nevertheless, our results strongly suggest that the observed phenotype is due to the influence of reduced FUBP1 levels on adult LT-HSC self-renewal, a discovery that will be further analyzed in future serial blood reconstitution assays.

The analysis of lineage contribution in the periphery of transplanted mice (Figures 3D and 3G) and the results from the colony-formation assays with total *Fubp1*$^{null/null}$ FL cells (Figure 1D) and prospectively isolated multipotent and committed progenitor populations (Figure S2) suggest that FUBP1 is not required for the lineage choice and differentiation of hematopoietic lineages. However, we did not test the full functionality of the mature blood cells lacking FUBP1. This observation correlates with the results of ex vivo colony-formation assays performed using adult *Fubp1*-knockdown HSPCs. All types of colonies were formed in the absence of FUBP1 expression (data not shown), which argues that FUBP1 is not required for such colony generation. In summary, it appears that FUBP1 fulfills a crucial stem cell-intrinsic function, enabling self-renewal in both fetal and adult LT-HSCs.

The Absence of FUBP1 Alters Target Gene Expression, Decelerates Proliferation, and Increases Cell Death Rates in LT-HSCs

Given that FUBP1 functions as a transcriptional regulator, we sought to identify genes involved in LT-HSC self-renewal that are controlled by FUBP1. Using qPCR, we assessed the expression levels of 34 candidate genes in adult LT-HSCs after transduction with *Fubp1* shRNA #2 or *scrambled* shRNA. The selected genes were either involved in the regulation of HSC self-renewal or represented known FUBP1 target genes (Figure 4A; Table S2). Several genes implicated in the regulation of HSC self-renewal, apoptosis, and proliferation were differentially expressed, including *HoxA10*, *p21*, and *Noxa*. The cell-cycle inhibitor gene *p21* and the pro-apoptotic *Bcl-2* gene family member *Noxa* have been previously identified as relevant FUBP1 target genes in HCCs (Rabenhorst et al., 2009), and their upregulation (3-fold for *p21* and 2.4-fold for *Noxa* mRNA) suggests increased cell death and decelerated proliferation, thereby preventing robust LT-HSC self-renewal and expansion. Indeed, cell culture experiments confirmed that LT-HSCs depleted of FUBP1 barely expanded during 7 days of culture, while control cell numbers increased exponentially (Figure 4B). A cell-cycle

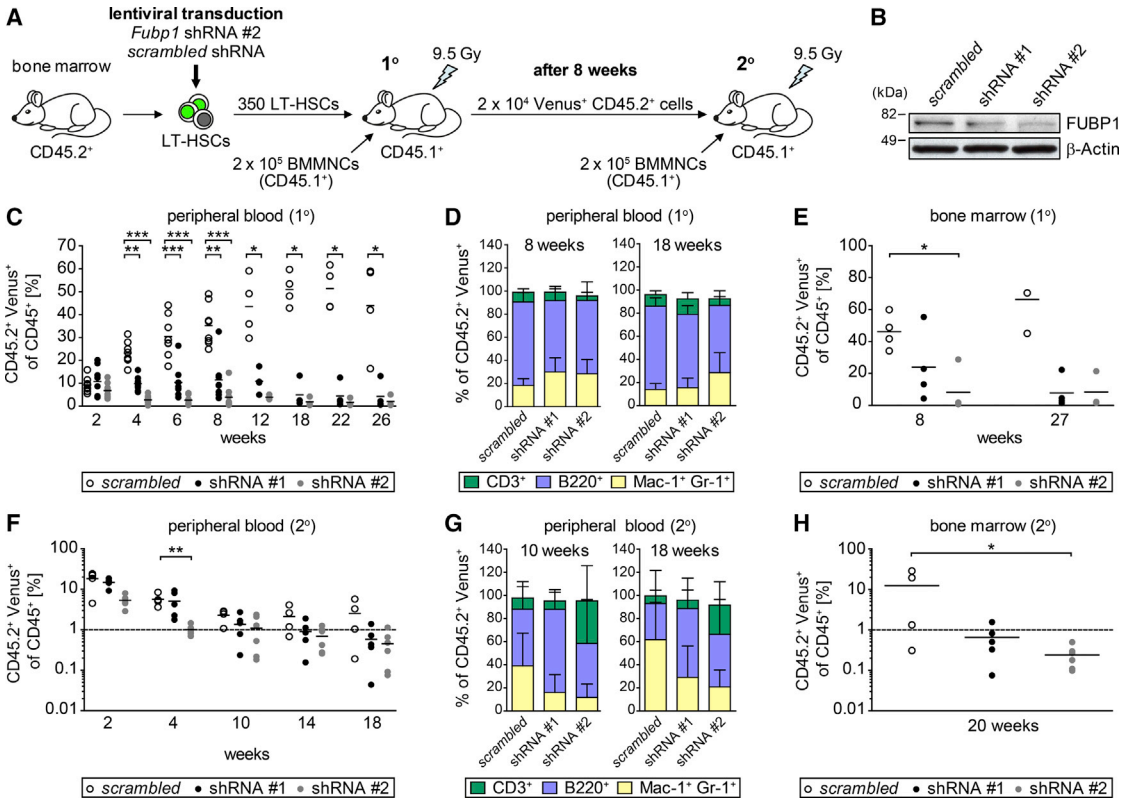

Figure 3. FUBP1 Is Intrinsically Required for Adult HSC Self-Renewal

(A) Experimental scheme.

(B) Western blot of lysates from MPPs lentivirally transduced with shRNAs.

(C and D) Multi-lineage donor cell reconstitution (CD45.2$^+$ Venus$^+$) of lethally irradiated recipient mice (eight per group; one experiment) after competitive transplantation of LT-HSCs transduced with *Fubp1* or *scrambled* shRNAs.

(E) BM analysis of recipient mice 8 (n = 4) and 27 (n = 3) weeks post-transplantation.

(F–H) Quantification of CD45.2$^+$ Venus$^+$ cells in the PB (F, *scrambled* and *Fubp1* shRNA #1: n = 5, *Fubp1* shRNA #2: n = 6) and BM (H, *scrambled* shRNA: n = 4, *Fubp1* shRNA #1: n = 5, *Fubp1* shRNA #2: n = 6) of secondary recipient mice. Test for statistical significance: Mann-Whitney; bar charts represent the mean and SD.

analysis of ex vivo cultured FUBP1-deficient LT-HSCs showed a significant decrease of cells in the S phase of the cell cycle and an increase of cells in the G_1 phase (Figures 4C and S4A), a result that verifies the reduced proliferation potential of FUBP1-deficient LT-HSCs.

Dysfunctional self-renewal of LT-HSCs leads to exhaustion of the hematopoietic system. To assess FUBP1-deficient LT-HSC impairment in self-renewal and long-term blood reconstitution and to validate the proposed functional changes caused by the absence of FUBP1, namely decreased proliferation and increased incidence of cell death, we continuously observed individual LT-HSCs and their progeny via video microscopy-based cell tracking (Rieger et al., 2009; Thalheimer et al., 2014). Adult LT-HSCs were lentivirally transduced with *Fubp1* shRNA #2 or *scrambled* shRNA and immediately subjected to time-lapse microscopy. The cells were monitored for 8 days to measure cell-cycle length and cell death events in each generation at single cell resolution (Figure 4D; Movies S1 and S2). The transduction of individual cells was determined by monitoring the co-expression of the fluorescent reporter protein Venus. *Fubp1* knockdown drastically increased the adult LT-HSC death rate in subsequent generations (generations 2 to 5; Figure 4E). Furthermore, the average time span between cell divisions of FUBP1-depleted LT-HSCs was significantly larger than in control cells of the same generation (Figure 4F). Overall, increased cell death rates and prolonged generation times resulted in the reduced expansion of FUBP1-deficient LT-HSCs in culture and most likely in the markedly reduced self-renewal capacity of LT-HSCs lacking functional FUBP1.

The minimal prerequisites for self-renewal of LT-HSCs are cell survival and division. In this study, we found that the single-stranded DNA-binding protein FUBP1 is absolutely essential for fetal and adult LT-HSC self-renewal, which acts by controlling the transcriptional network that governs survival and proliferation of LT-HSCs (see working model presented in Figure S4B). Interestingly, all committed progenitors and mature blood cells are generated in the absence of FUBP1 (although we did not investigate the functionality of the differentiated cells), which suggests that FUBP1 plays a specific role in the hematopoietic cell type with extensive self-renewal ability, namely

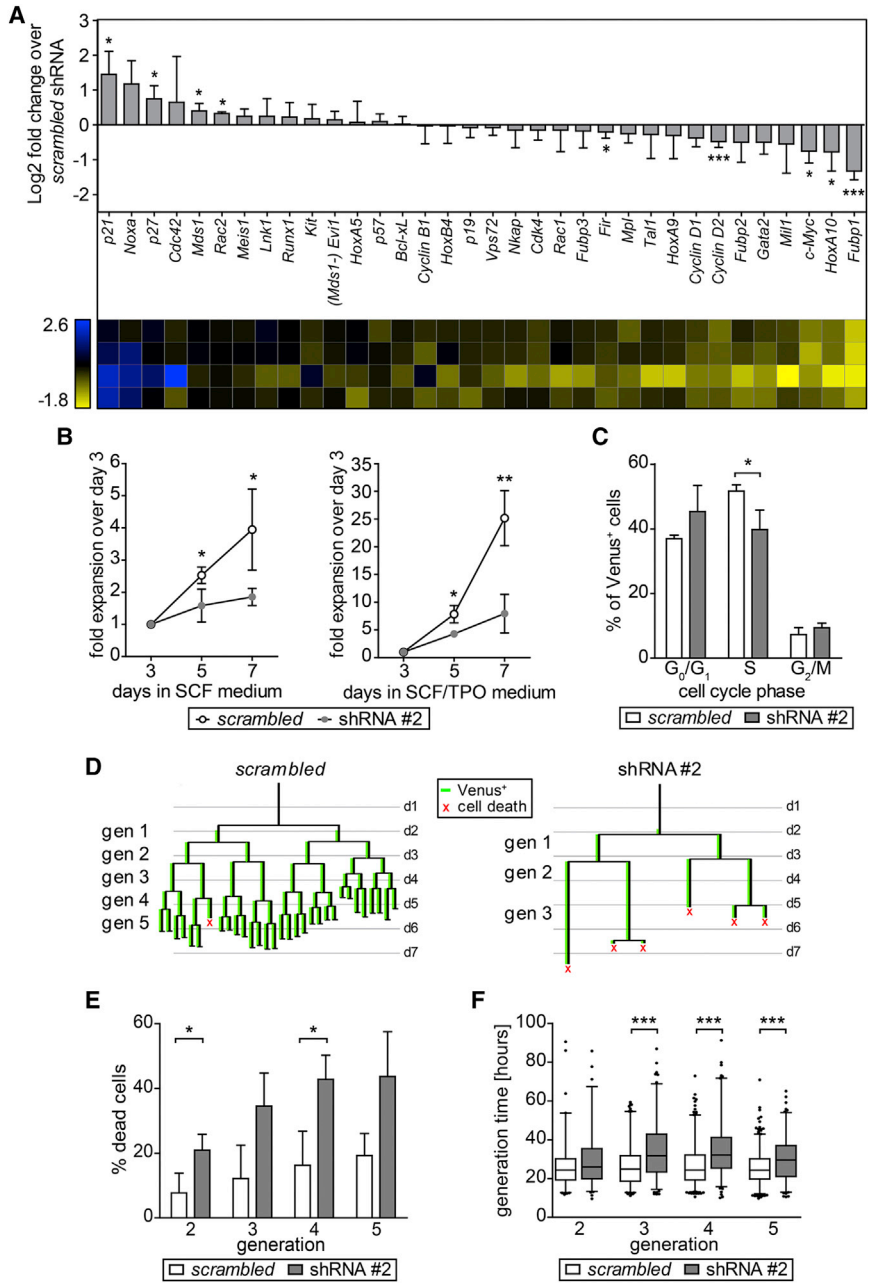

Figure 4. The Transcriptional Regulator FUBP1 Promotes Proliferation and Survival of LT-HSCs, Thereby Enabling LT-HSC Self-Renewal

(A) qPCR of FACS-isolated adult LT-HSCs transduced with *scrambled* or *Fubp1* shRNA #2. Relative expression levels (log_2; fold change between *Fubp1* shRNA #2- and *scrambled* shRNA-transduced HSCs) were normalized to the geometric mean of six housekeeping genes (*Hprt*, *β-Act*, *Pum1*, *Gusb*, *B2m*, and *Gapdh*). Data are presented as the mean and SD and with a heatmap (four independent experiments).

(B) Culture of lentivirally transduced LT-HSCs, three independent experiments.

(C) Cell-cycle analysis of ex vivo cultured lentivirally transduced LT-HSCs, three independent experiments.

(D) Representative pedigrees of two tracked LT-HSCs that had been transduced with *scrambled* shRNA (left) or *Fubp1* shRNA #2 (right).

(E and F) Cell tracking revealed increased cell death rates (E) and prolonged generation times (F) upon *Fubp1* knockdown (three independent experiments). Numbers of tracked cells for each generation: 173–639 *scrambled* shRNA-transduced cells and 189–268 *Fubp1* shRNA#2-transduced cells. Test for statistical significance: unpaired Student's t test. Data are represented as the mean and SD or as boxes (25%–75%) and whiskers with 2.5–97.5 percentile.

LT-HSCs. However, *Fubp1* mRNA expression within HSPCs is not restricted to LT-HSCs (Figure S4C).

Our LT-HSC expression analysis reveals that several genes implicated in LT-HSC self-renewal, including *c-myc*, *p21*, and *Noxa*, are deregulated in the absence of FUBP1 (Figure 4A). *c-myc* was the first identified direct FUBP1 target gene (Duncan et al., 1994), and we confirmed significant downregulation of *c-myc* mRNA expression in adult *Fubp1* knockdown LT-HSCs. *c-myc* plays an important role in hematopoiesis as well as HSC self-renewal and differentiation (Laurenti et al., 2009). However, the reported accumulation of non-functional LT-HSCs in tissue-specific *c-myc*-knockout embryos (Dubois et al., 2008) and adult mice (Wilson et al., 2004) contrasts with our observations in FUBP1-deficient embryos and mice transplanted with adult *Fubp1*-knockdown HSCs, challenging *c-myc* as the most relevant target gene to explain the defective self-renewal of FUBP1-deficient HSCs. With *p21* and *Noxa*, we identified two genes controlling cell-cycle progression and cell death that are suppressed by FUBP1 in LT-HSCs. p21 binds to cyclin-dependent kinase (CDK)/cyclin complexes, thereby inhibiting CDK activity and cell-cycle progression (Warfel and El-Deiry, 2013). NOXA belongs to the pro-apoptotic group of BH3 domain-only proteins, a subclass of the BCL-2 family (Ploner et al., 2008). In previous studies, we have demonstrated that both genes are suppressed upon frequent overexpression of FUBP1 in HCCs (Rabenhorst et al., 2009). Furthermore, downregulation of *FUBP1* in HCC cell lines increased apoptosis sensitivity and slowed cell-cycle progression, thereby leading to reduced tumorigenicity. We observed a similar pro-apoptotic and anti-proliferative phenotype in LT-HSCs lacking FUBP1, which strongly indicates that the suppression of both genes to levels below a certain threshold is instrumental for HSC self-renewal and expansion. Conversely, overexpression of both genes was shown to interfere with normal LT-HSC function: homozygous

Ptpn11$^{-/-}$ mice deficient in Src homology 2 domain-containing phosphatase 2 (SHP2) showed a rapid loss of LT-HSCs due to apoptosis concomitant with increased NOXA expression (Chan et al., 2011), and the accumulation of p21 and p27 in GATA-2-overexpressing HSPCs suppressed cytokine-dependent growth (Ezoe et al., 2002). Our results show that self-renewal of HSCs not only requires the activation, but also the repression of certain gene programs.

FUBP1 is absolutely essential for LT-HSC self-renewal in embryos and adult organisms. This contrasts with other factors that have been shown to be specifically important for either fetal or adult HSC self-renewal, such as TAL1 (Mikkola et al., 2003), SOX17 (Kim et al., 2007), or RUNX1 (Ichikawa et al., 2004). Indeed, fundamental differences in the molecular state of fetal and adult LT-HSCs as well as the regulatory transcriptional networks that govern LT-HSC self-renewal and maintain their stemness and repopulating capacity have been described (Wilkinson and Göttgens, 2013).

The observation that FUBP1 plays a central role in fetal and adult LT-HSC self-renewal adds another level of complexity to the regulation of transcription by DNA structure. The accessibility of the melted single-strand DNA element *FUSE* is the first prerequisite for FUBP1 to become involved in gene regulation upon binding to *FUSE* sites in the vicinity of gene promoters. Therefore, FUBP1 represents the prototype of molecular switches that translate structural DNA information into the activation or inhibition of promoters regulating LT-HSC self-renewal. The integration of FUBP1 expression and function and its regulation by intrinsic and extrinsic factors warrants future investigations to further our understanding of self-renewal mechanisms for the longstanding goal of therapeutic LT-HSC expansion. It will be intriguing to find out whether FUBP1 fulfills a similar function for the self-renewal of other somatic or embryonic stem cells. Furthermore, the oncogenic potential of FUBP1 overexpression has already been demonstrated in human HCCs (Malz et al., 2009; Rabenhorst et al., 2009) and other tumor entities (data not shown), and *FUBP1* mRNA levels were shown significantly elevated in leukemia stem cell-enriched cell populations (Eppert et al., 2011). Thus, it will be of great interest to understand the role that FUBP1 plays in tumor-initiating cells (cancer stem cells).

EXPERIMENTAL PROCEDURES

Mouse Lines

Two heterozygous *Fubp1*$^{null/+}$ gene trap mouse strains were established via injection of the ES cell clones A033A08 (GT 1, gene trap integration into *Fubp1* intron 18; oligonucleotides used for genotyping were 5′-CTGGGTTCAAATCC CACTAC-3′ [primer 5′], 5′-TACCTAGCTCACCACTCTTC-3′ [primer wt-3′] and 5′-ACGGGTTCTTCTGTTAGTCC-3′ [primer trap-3′]) and 5SE293C09 (*GT 2*, gene trap integration into *Fubp1* intron 1; oligonucleotides used for genotyping were 5′-CCTGGCAGGTCTCTTGAGTT-3′ [primer 5′-2], 5′-CCAAAGGGTCC TACATGGAA-3′ [primer wt-3′-2] and 5′-AGTGATTGACTACCCGTCAGC-3′ [primer trap-3′-2]) obtained from the International Gene Trap Consortium (IGTC; http://www.genetrap.org/index.html). The GT 1 strain expresses a non-functional fusion protein consisting of aa 1-589 of FUBP1, the β-galactosidase (β-Gal) and the aminoglycoside 3′-phosphotransferase (APT) protein (Figure 1B, left). The GT 2 strain expressed no FUBP1 protein sequence (Figure 1B, right). The mutant animals were bred into the *C57Bl/6J* strain (*Charles River*) before analysis. CD45.1^{+} *B6.SJL* mice were purchased from Jackson Laboratory. All mice were bred and maintained under specific pathogen-free conditions in the animal facility at the Georg-Speyer-Haus. Experiments were performed in accordance with German animal welfare legislation and were approved by the relevant authorities (Regierungspräsidium Darmstadt).

Isolation of BMCs and Lineage Depletion

BMCs were isolated from the femurs and the tibias by flushing the bones using a syringe with a blunt needle or by crushing the femurs, tibias, and sternums in sterile PBS/2% fetal bovine serum (FBS). After flushing, mononuclear cells from murine BM were isolated via density gradient centrifugation using *Histopaque 1083* (Sigma-Aldrich) according to the manufacturer's instructions. Lineage depletion of FL cells and BMCs was performed using the EasySep Kit (Stem Cell Technologies) according to the manufacturer's protocol. Biotinylated antibodies against B220 (RA3-6B2), CD3 (145-2C11), CD19 (eBio1D3), CD41 (eBioMWReg30), Gr-1 (RB6-8C5), Mac-1 (M1/70), and Ter119 (TER-119) were used to isolate lineage-depleted cells. For FL cell lineage depletion, anti-Mac-1 (Morrison et al., 1995), and anti-CD41 antibodies were excluded from the antibody cocktail (see Table S1 for detailed antibody information).

Staining and Sorting of Fetal and Adult HSPC Populations

Fetal and adult LT-HSCs were isolated from FLs and adult BM, respectively. The cells were quantified using trypan blue and a hemocytometer, and the cells were incubated with the appropriate antibodies in PBS (pH 7.4) containing 10% FBS, 1 mM EDTA, and 0.1% sodium azide. FL HSPC staining was performed using the following antibodies against Sca-1 (D7), CD117 (2B8), CD48 (HM48.1), CD150 (TC15-12F12.2), and Mac-1 (M1/70). For BM HSPCs, antibodies against Sca-1 (D7), CD117 (2B8), CD48 (HM48.1), CD150 (TC15-12F12.2), and CD34 (RAM34) were used. Streptavidin was added for detection of remaining lineage^{+} cells (lineage biotin cocktail; see above). For progenitor analysis of transplanted BM, anti-CD45.1 (A20) and anti-CD45.2 (104) antibodies were included in addition to the above mentioned antibodies. Flow cytometric analysis was performed using a FACSCalibur or a FACSCanto II (Becton Dickinson), and cells were sorted using a FACSAria I (Becton Dickinson). Gating of BM HSPC populations was done as shown in (Thalheimer et al., 2014). Living cells after sorting were counted by trypan blue exclusion. Data analysis was carried out using FACS Diva, CellQuest (Becton Dickinson), and FlowJo (Tree Star) software.

Flow Cytometry for Donor Cell Engraftment in PB

Whole mouse blood samples (50 μl) were harvested, and erythrocytes were lysed in ACK lysis buffer (GIBCO Life Technologies). After washing, the cells were used for antibody staining (Gr-1 [RB6-8C5], Mac-1 [M1/70], CD3 [145-2C11], B220 [RA3-6B2], CD45.1 [A20], and CD45.2 [104]) and flow cytometric analysis.

Competitive Transplantation

CD45.1^{+} *B6.SJL* recipient mice were lethally irradiated with 9.5 Gy (Biobeam 2000). CD45.2^{+} FL cells or fluorescence-activated cell sorting (FACS)-sorted adult HSCs (1-day post-transduction) resuspended in PBS were injected into the tail vein together with 2 × 10^5 non-fractionated BMCs isolated from CD45.1^{+} *B6.SJL* mice.

Quantitative Real-Time PCR

Lentivirally transduced Venus^{+} CD48^{-} HSCs were sorted directly into lysis buffer 2 days after transduction of LT-HSCs. cDNA synthesis, cDNA preamplification, and *TaqMan* qPCR assays were then carried out using a Roche *LightCycler480* PCR system and the TaqMan PreAmp Cells-to-C_T Kit (Life Technologies) according to the manufacturer's instructions. *TaqMan* Gene Expression Assays were purchased from Life Technologies (see Table S2). Data analysis was performed using the $\Delta\Delta C_T$-method (Schefe et al., 2006). The geometric mean of six housekeeping genes (*Hprt*, *β-Act*, *Pum1*, *Gusb*, *B2m*, and *Gapdh*) was used to normalize the data. The $\log_2$ fold change of all genes of interest was calculated to compare *Fubp1* shRNA #2-transduced knockdown and *scrambled* shRNA-transduced control cells.

Colony-Forming Unit Assay

For colony-formation assays, 5 × 10^3 total FL cells were mixed with MethoCult methylcellulose medium (M3434, Stem Cell Technologies) and then plated according to the manufacturer' s instructions. The colonies were scored via microscopy at day 11.

Time-Lapse Imaging

FACS-sorted LT-HSCs (30–50 cells/per well) were cultured in 24-well plates (SFEM medium, 100 ng/ml stem cell factor [SCF] and thrombopoietin [TPO]) equipped with silicon culture inserts (IBIDI) and immediately transduced with lentiviral particles (MOI 300). The plates were gas-tight sealed with adhesive tape after 5% CO_2 saturation. Microscopy was performed using a Cell Observer (Zeiss) at 37°C. Phase contrast images were acquired every 2–3 min using a 10× phase contrast objective (Zeiss) and an AxioCamHRm camera (at 1,388 × 1,040 pixel resolution) with a self-written VBA module remote controlling the Zeiss AxioVision 4.8 software. Fluorescence was detected every 1–2 hr using HXP illumination (Osram) and a filter set for EYFP (F46-003, AHF Analysetechnik).

Cell Tracking

Cell tracking was performed as previously described (Rieger et al., 2009; Thalheimer et al., 2014) until the fate of all progeny in the fifth generation was determined or until cells had died.

Ex Vivo Culture of LT-HSCs

FACS-sorted LT-HSCs (100 cells per well) were cultured in 96-well plates after lentiviral transduction (MOI = 300) in SFEM medium (StemCell Technologies) supplemented with either SCF or SCF and TPO (100 ng/ml, Peprotech) at 5% CO_2 and 37°C. On days 3, 5 and 7, cells were counted and analyzed via flow cytometry for Venus fluorescence.

BrdU Cell Proliferation Assay

For cell-cycle analysis, the BrdU Flow Kit (BD Pharmingen) was used according to the manufacturer's instructions. LT-HSCs were transduced as described above and cultured in SFEM medium (Stem Cell Technologies) supplemented with 100 ng/ml SCF and TPO (Peprotech). On day 3 after transduction, LT-HSCs were pulsed with BrdU for 45 min. 7-AAD was used to quantify total DNA amounts. Flow cytometric analysis of $Venus^+$ cells was performed using a LSR Fortessa (Becton Dickinson).

Statistical Analyses

The statistical analyses indicated in the figure legends were performed with Prism 5 for Mac OS X, GraphPad Prism Software; *$p < 0.05$, **$p < 0.01$, ***$p < 0.001$.

Additional information about experimental procedures is presented in the Supplemental Information.

SUPPLEMENTAL INFORMATION

Supplemental Information includes Supplemental Experimental Procedures, four figures, two tables, and two movies and can be found with this article online at http://dx.doi.org/10.1016/j.celrep.2015.05.038.

AUTHOR CONTRIBUTIONS

U.R., F.B.T., K.G., M.K., and S.B. participated in the acquisition, analysis, and interpretation of data. D.S.K., F.V., H.-H.A., T.S., F.S., and H.v.M. handled material support and acquisition, analysis, and interpretation of data. M.A.R. was in charge of experimental design, analysis, and interpretation of data and drafting and critical revision of the manuscript for important intellectual content. M.Z. was responsible for experimental design, analysis, and interpretation of data and drafting of the manuscript. All authors have approved the final version of the manuscript.

ACKNOWLEDGMENTS

We are thankful to Susanne Bösser, Claudia Jourdan, and Sabrina Bothur for excellent technical assistance as well as Tefik Merovci for support with FACS cell sorting, Eva Herrmann (Institute for Biostatistics and Mathematical Modelling, Goethe University) for advice on the statistical analysis of our results, and Boris Brill for help with the transplantations. This work is supported by grants provided by the Deutsche Krebshilfe (project no. 109327), the LOEWE Center for Cell and Gene Therapy (HMWK III L 4-518/17.004 (2013)), the German Research Foundation (ZO 110/7-1) and the Georg-Speyer-Haus (funded by the German Federal Ministry of Health [BMG] and the Ministry of Higher Education, Research and the Arts of the state of Hessen [HMWK]).

Received: November 14, 2014
Revised: May 8, 2015
Accepted: May 23, 2015
Published: June 18, 2015

REFERENCES

Chan, G., Cheung, L.S., Yang, W., Milyavsky, M., Sanders, A.D., Gu, S., Hong, W.X., Liu, A.X., Wang, X., Barbara, M., et al. (2011). Essential role for Ptpn11 in survival of hematopoietic stem and progenitor cells. Blood *117*, 4253–4261.

Chung, H.J., and Levens, D. (2005). c-myc expression: keep the noise down!. Mol. Cells *20*, 157–166.

Dubois, N.C., Adolphe, C., Ehninger, A., Wang, R.A., Robertson, E.J., and Trumpp, A. (2008). Placental rescue reveals a sole requirement for c-Myc in embryonic erythroblast survival and hematopoietic stem cell function. Development *135*, 2455–2465.

Duncan, R., Bazar, L., Michelotti, G., Tomonaga, T., Krutzsch, H., Avigan, M., and Levens, D. (1994). A sequence-specific, single-strand binding protein activates the far upstream element of c-myc and defines a new DNA-binding motif. Genes Dev. *8*, 465–480.

Eppert, K., Takenaka, K., Lechman, E.R., Waldron, L., Nilsson, B., van Galen, P., Metzeler, K.H., Poeppl, A., Ling, V., Beyene, J., et al. (2011). Stem cell gene expression programs influence clinical outcome in human leukemia. Nat. Med. *17*, 1086–1093.

Ezoe, S., Matsumura, I., Nakata, S., Gale, K., Ishihara, K., Minegishi, N., Machii, T., Kitamura, T., Yamamoto, M., Enver, T., and Kanakura, Y. (2002). GATA-2/estrogen receptor chimera regulates cytokine-dependent growth of hematopoietic cells through accumulation of p21(WAF1) and p27(Kip1) proteins. Blood *100*, 3512–3520.

Ichikawa, M., Asai, T., Saito, T., Seo, S., Yamazaki, I., Yamagata, T., Mitani, K., Chiba, S., Ogawa, S., Kurokawa, M., and Hirai, H. (2004). AML-1 is required for megakaryocytic maturation and lymphocytic differentiation, but not for maintenance of hematopoietic stem cells in adult hematopoiesis. Nat. Med. *10*, 299–304.

Kim, I., He, S., Yilmaz, O.H., Kiel, M.J., and Morrison, S.J. (2006). Enhanced purification of fetal liver hematopoietic stem cells using SLAM family receptors. Blood *108*, 737–744.

Kim, I., Saunders, T.L., and Morrison, S.J. (2007). Sox17 dependence distinguishes the transcriptional regulation of fetal from adult hematopoietic stem cells. Cell *130*, 470–483.

Laurenti, E., Wilson, A., and Trumpp, A. (2009). Myc's other life: stem cells and beyond. Curr. Opin. Cell Biol. *21*, 844–854.

Liu, J., Chung, H.J., Vogt, M., Jin, Y., Malide, D., He, L., Dundr, M., and Levens, D. (2011). JTV1 co-activates FBP to induce USP29 transcription and stabilize p53 in response to oxidative stress. EMBO J. *30*, 846–858.

Malz, M., Weber, A., Singer, S., Riehmer, V., Bissinger, M., Riener, M.O., Longerich, T., Soll, C., Vogel, A., Angel, P., et al. (2009). Overexpression of far upstream element binding proteins: a mechanism regulating proliferation and migration in liver cancer cells. Hepatology *50*, 1130–1139.

Mikkola, H.K., Klintman, J., Yang, H., Hock, H., Schlaeger, T.M., Fujiwara, Y., and Orkin, S.H. (2003). Haematopoietic stem cells retain long-term

repopulating activity and multipotency in the absence of stem-cell leukaemia SCL/tal-1 gene. Nature *421*, 547–551.

Morrison, S.J., Hemmati, H.D., Wandycz, A.M., and Weissman, I.L. (1995). The purification and characterization of fetal liver hematopoietic stem cells. Proc. Natl. Acad. Sci. USA *92*, 10302–10306.

Nishino, T., Osawa, M., and Iwama, A. (2012). New approaches to expand hematopoietic stem and progenitor cells. Expert Opin. Biol. Ther. *12*, 743–756.

Orkin, S.H., and Zon, L.I. (2008). Hematopoiesis: an evolving paradigm for stem cell biology. Cell *132*, 631–644.

Pietras, E.M., Warr, M.R., and Passegué, E. (2011). Cell cycle regulation in hematopoietic stem cells. J. Cell Biol. *195*, 709–720.

Ploner, C., Kofler, R., and Villunger, A. (2008). Noxa: at the tip of the balance between life and death. Oncogene *27* (*1*), S84–S92.

Qiu, J., Papatsenko, D., Niu, X., Schaniel, C., and Moore, K. (2014). Divisional history and hematopoietic stem cell function during homeostasis. Stem Cell Reports *2*, 473–490.

Rabenhorst, U., Beinoraviciute-Kellner, R., Brezniceanu, M.L., Joos, S., Devens, F., Lichter, P., Rieker, R.J., Trojan, J., Chung, H.J., Levens, D.L., and Zörnig, M. (2009). Overexpression of the far upstream element binding protein 1 in hepatocellular carcinoma is required for tumor growth. Hepatology *50*, 1121–1129.

Rieger, M.A., and Schroeder, T. (2012). Hematopoiesis. Cold Spring Harbor Perspect. Biol. *4*, a008250.

Rieger, M.A., Hoppe, P.S., Smejkal, B.M., Eitelhuber, A.C., and Schroeder, T. (2009). Hematopoietic cytokines can instruct lineage choice. Science *325*, 217–218.

Samokhvalov, I.M., Samokhvalova, N.I., and Nishikawa, S. (2007). Cell tracing shows the contribution of the yolk sac to adult haematopoiesis. Nature *446*, 1056–1061.

Schefe, J.H., Lehmann, K.E., Buschmann, I.R., Unger, T., and Funke-Kaiser, H. (2006). Quantitative real-time RT-PCR data analysis: current concepts and the novel "gene expression's CT difference" formula. J. Mol. Med. *84*, 901–910.

Schlaeger, T.M., Mikkola, H.K., Gekas, C., Helgadottir, H.B., and Orkin, S.H. (2005). Tie2Cre-mediated gene ablation defines the stem-cell leukemia gene (SCL/tal1)-dependent window during hematopoietic stem-cell development. Blood *105*, 3871–3874.

Thalheimer, F.B., Wingert, S., De Giacomo, P., Haetscher, N., Rehage, M., Brill, B., Theis, F.J., Hennighausen, L., Schroeder, T., and Rieger, M.A. (2014). Cytokine-regulated GADD45G induces differentiation and lineage selection in hematopoietic stem cells. Stem Cell Reports *3*, 34–43.

Warfel, N.A., and El-Deiry, W.S. (2013). p21WAF1 and tumourigenesis: 20 years after. Curr. Opin. Oncol. *25*, 52–58.

Wilkinson, A.C., and Göttgens, B. (2013). Transcriptional regulation of haematopoietic stem cells. Adv. Exp. Med. Biol. *786*, 187–212.

Wilson, A., Murphy, M.J., Oskarsson, T., Kaloulis, K., Bettess, M.D., Oser, G.M., Pasche, A.C., Knabenhans, C., Macdonald, H.R., and Trumpp, A. (2004). c-Myc controls the balance between hematopoietic stem cell self-renewal and differentiation. Genes Dev. *18*, 2747–2763.

Wilson, A., Laurenti, E., Oser, G., van der Wath, R.C., Blanco-Bose, W., Jaworski, M., Offner, S., Dunant, C.F., Eshkind, L., Bockamp, E., et al. (2008). Hematopoietic stem cells reversibly switch from dormancy to self-renewal during homeostasis and repair. Cell *135*, 1118–1129.

Wohrer, S., Knapp, D.J., Copley, M.R., Benz, C., Kent, D.G., Rowe, K., Babovic, S., Mader, H., Oostendorp, R.A., and Eaves, C.J. (2014). Distinct stromal cell factor combinations can separately control hematopoietic stem cell survival, proliferation, and self-renewal. Cell Rep. *7*, 1956–1967.

Cell Reports

Supplemental Information

Single-Stranded DNA-Binding Transcriptional Regulator FUBP1 Is Essential for Fetal and Adult Hematopoietic Stem Cell Self-renewal

Uta Rabenhorst, Frederic B. Thalheimer, Katharina Gerlach, Marek Kijonka, Stefanie Böhm, Daniela S. Krause, Franz Vauti, Hans-Henning Arnold, Timm Schroeder, Frank Schnütgen, Harald von Melchner, Michael A. Rieger, and Martin Zörnig

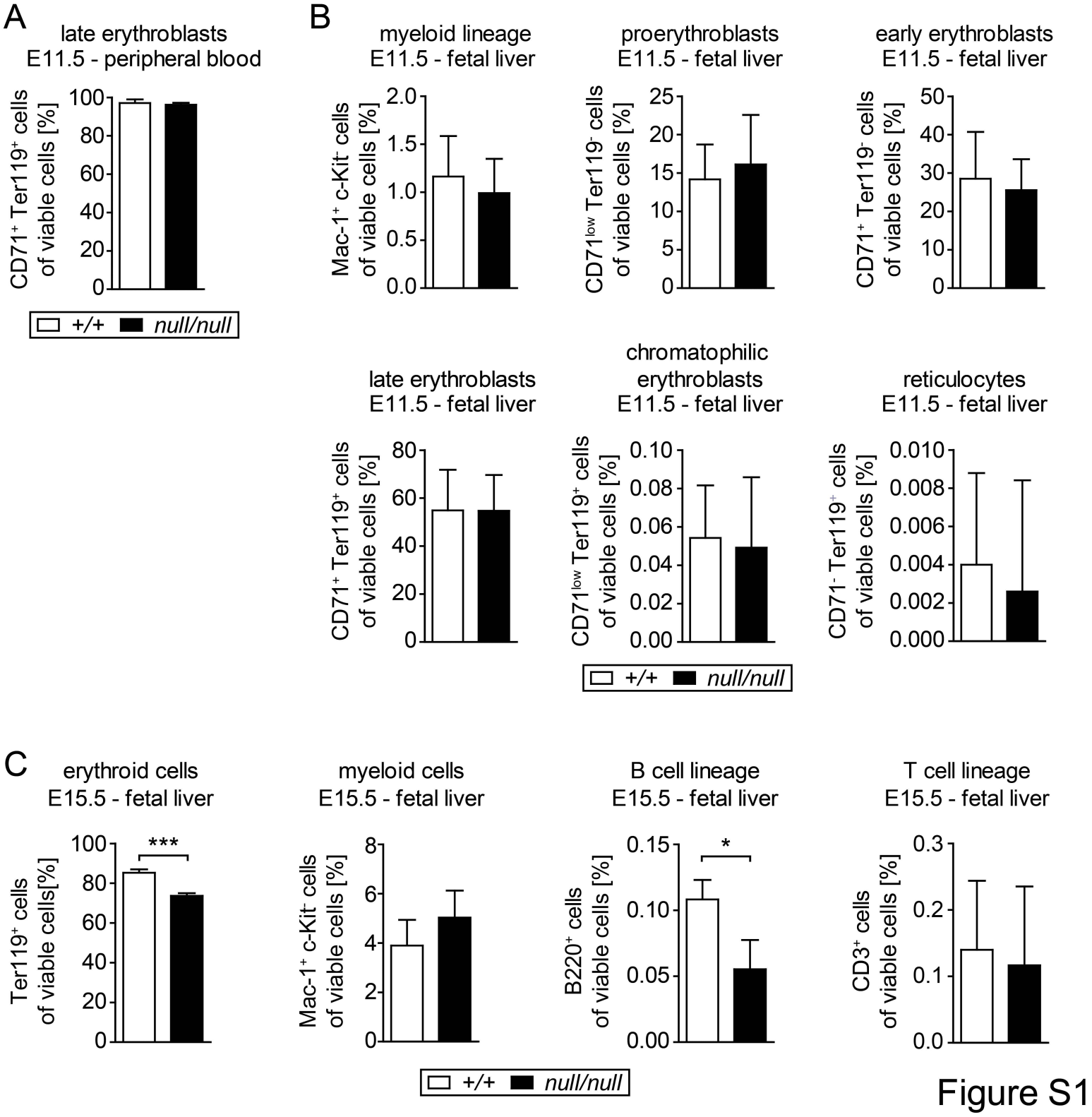
A
late erythroblasts
E11.5 - peripheral blood
CD71+ Ter119+ cells of viable cells [%]
100
80
60
40
20
0
+/+
null/null
B
myeloid lineage
E11.5 - fetal liver
Mac-1+ c-Kit- cells of viable cells [%]
2.0
1.5
1.0
0.5
0.0
proerythroblasts
E11.5 - fetal liver
CD71low Ter119- cells of viable cells [%]
25
20
15
10
5
0
early erythroblasts
E11.5 - fetal liver
CD71+ Ter119- cells of viable cells [%]
50
40
30
20
10
0
late erythroblasts
E11.5 - fetal liver
CD71+ Ter119+ cells of viable cells [%]
80
60
40
20
0
chromatophilic erythroblasts
E11.5 - fetal liver
CD71low Ter119+ cells of viable cells [%]
0.10
0.08
0.06
0.04
0.02
0.00
reticulocytes
E11.5 - fetal liver
CD71- Ter119+ cells of viable cells [%]
0.010
0.008
0.006
0.004
0.002
0.000
+/+
null/null
C
erythroid cells
E15.5 - fetal liver
Ter119+ cells of viable cells[%]
***
100
80
60
40
20
0
myeloid cells
E15.5 - fetal liver
Mac-1+ c-Kit- cells of viable cells [%]
8
6
4
2
0
B cell lineage
E15.5 - fetal liver
B220+ cells of viable cells [%]
*
0.15
0.10
0.05
0.00
T cell lineage
E15.5 - fetal liver
CD3+ cells of viable cells [%]
0.3
0.2
0.1
0.0
+/+
null/null

Figure S1

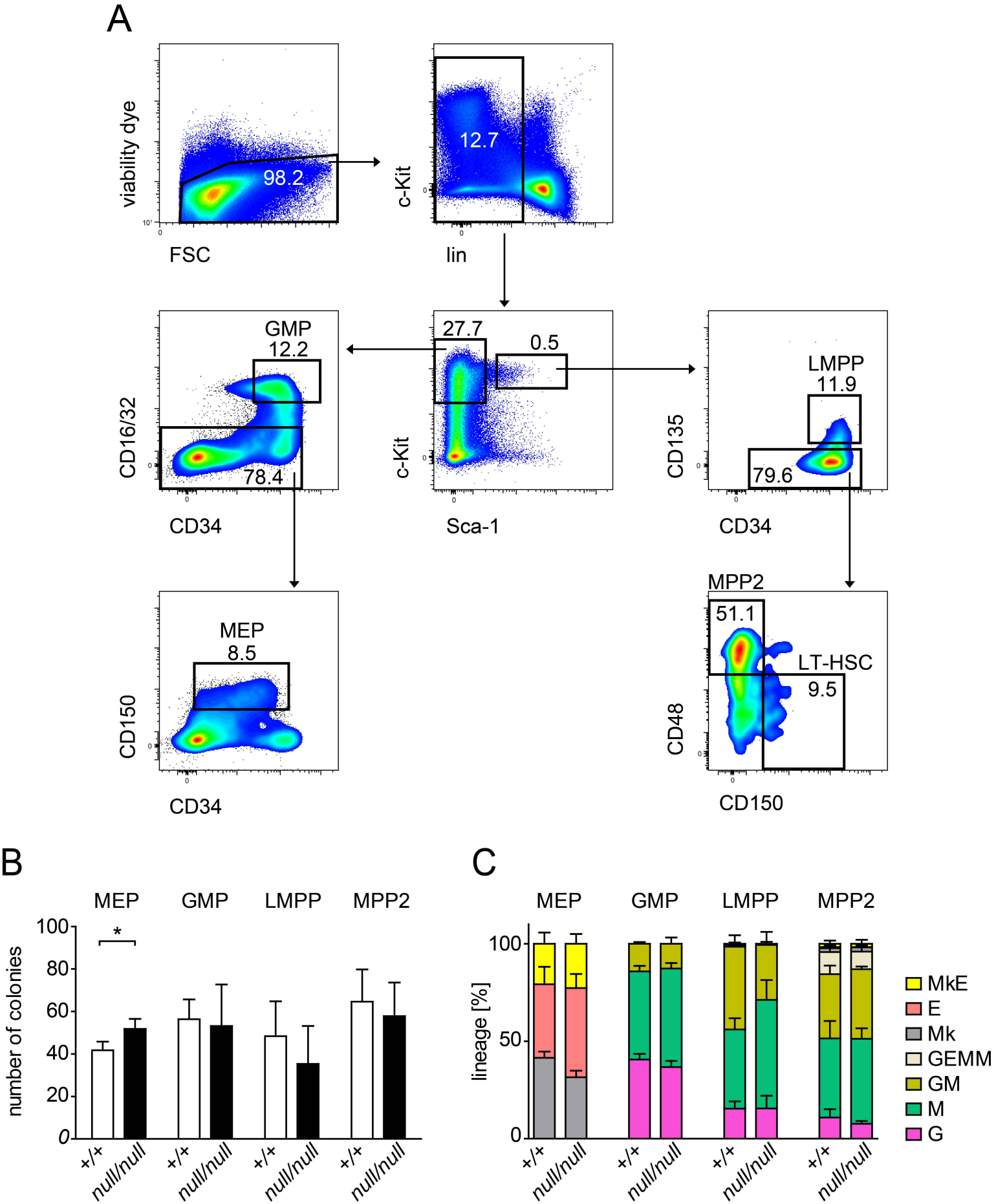
A
viability dye
98.2
FSC
c-Kit
12.7
lin
GMP
12.2
CD16/32
78.4
CD34
27.7
0.5
c-Kit
Sca-1
LMPP
11.9
CD135
79.6
CD34
MEP
8.5
CD150
CD34
MPP2
51.1
LT-HSC
9.5
CD48
CD150
B
MEP
GMP
LMPP
MPP2
number of colonies
100
80
60
40
20
0
*
+/+
null/null
C
MEP
GMP
LMPP
MPP2
lineage [%]
100
50
0
MkE
E
Mk
GEMM
GM
M
G

Figure S2

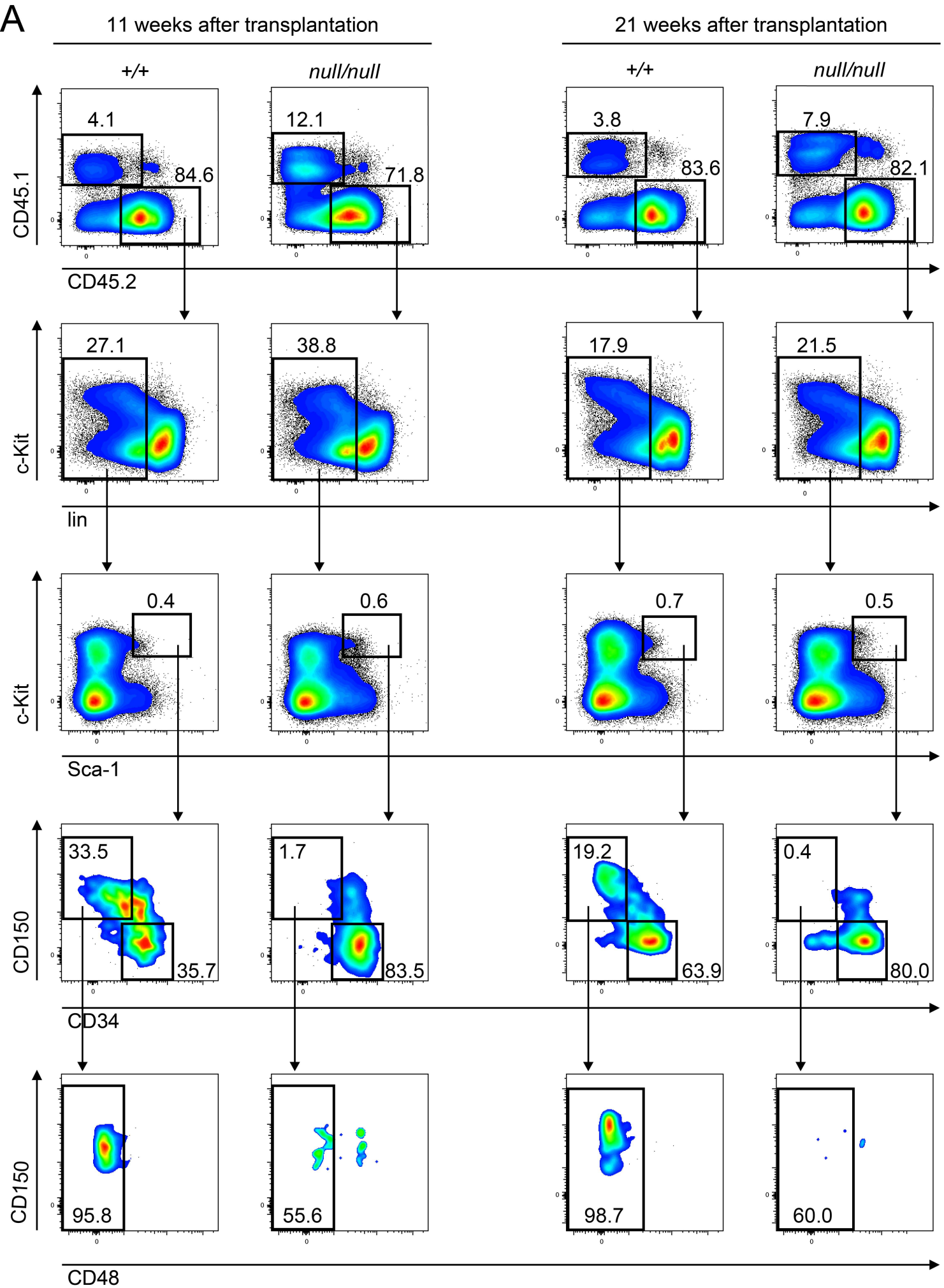
A
11 weeks after transplantation
21 weeks after transplantation
+/+
null/null
+/+
null/null
CD45.1
CD45.2
4.1
84.6
12.1
71.8
3.8
83.6
7.9
82.1
c-Kit
lin
27.1
38.8
17.9
21.5
c-Kit
Sca-1
0.4
0.6
0.7
0.5
CD150
CD34
33.5
35.7
1.7
83.5
19.2
63.9
0.4
80.0
CD150
CD48
95.8
55.6
98.7
60.0

Figure S3

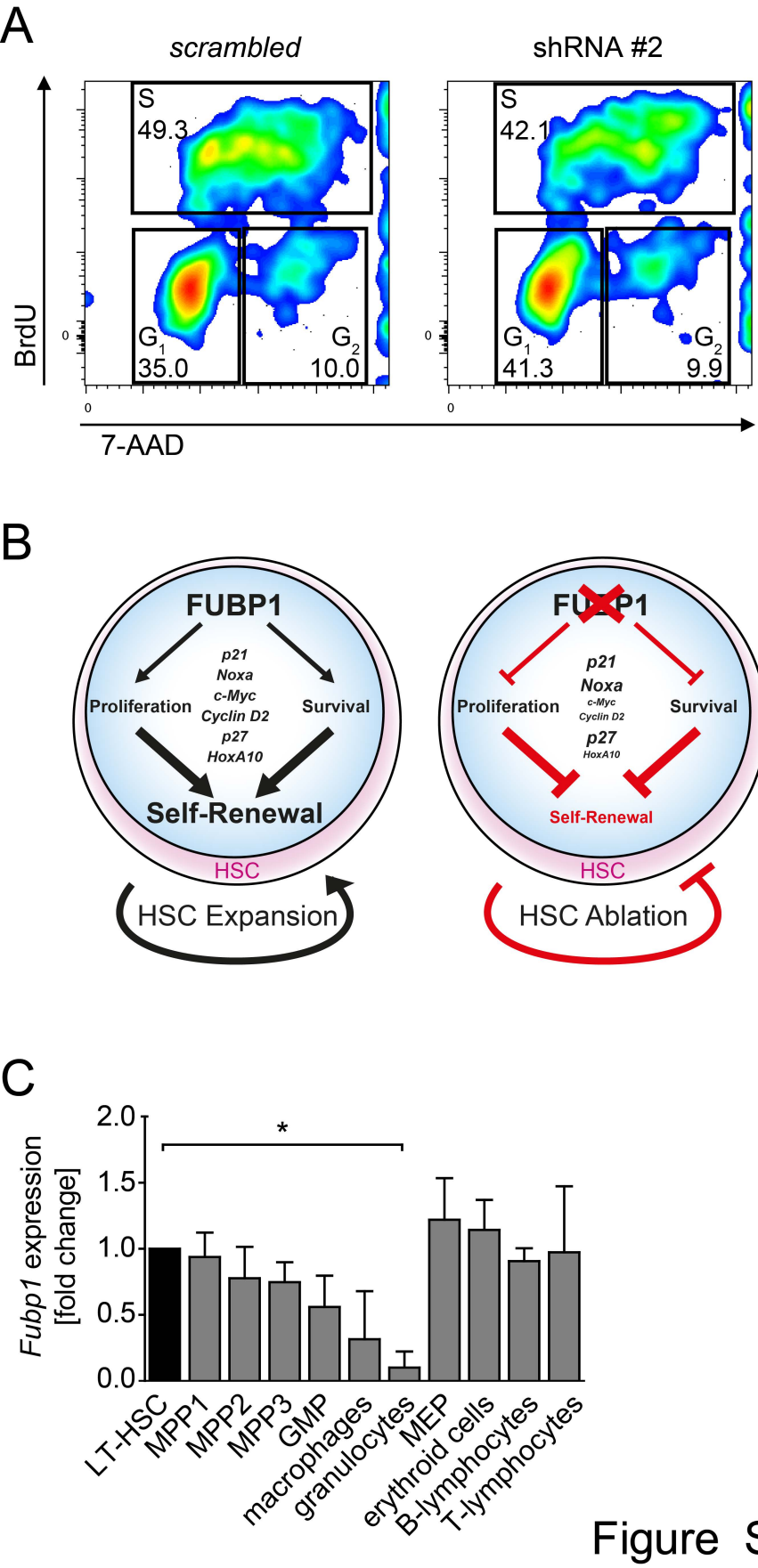
A
scrambled
shRNA #2
S
49.3
G1
35.0
G2
10.0
S
42.1
G1
41.3
G2
9.9
BrdU
7-AAD
B
FUBP1
p21
Noxa
c-Myc
Cyclin D2
p27
HoxA10
Proliferation
Survival
Self-Renewal
HSC
HSC Expansion
FUBP1
p21
Noxa
c-Myc
Cyclin D2
p27
HoxA10
Proliferation
Survival
Self-Renewal
HSC
HSC Ablation
C
Fubp1 expression
[fold change]
2.0
1.5
1.0
0.5
0.0
*
LT-HSC
MPP1
MPP2
MPP3
GMP
macrophages
granulocytes
MEP
erythroid cells
B-lymphocytes
T-lymphocytes

Figure S4

Supplemental Figure Legends

Figure S1: Lineage distribution in peripheral blood and fetal liver of E11.5 and E15.5 wildtype and *Fubp1*$^{null/null}$ embryos, related to Figure 1. (A, B) Primitive hematopoiesis appears normal in the absence of FUBP1. Peripheral blood (A) and fetal liver (B) isolated from E11.5 GT1 +/+ (wn=7) and *null/null* (FUBP1-deficient, n=5) embryos were analyzed for myeloid and erythroid lineages via flow cytometry. Dead cells were excluded from the analysis. The diagrams present the relative flow cytometric quantification of 2 independent experiments; data are represented as the mean and standard deviation (SD). (C) Only mild changes in the proportion of the main hematopoietic lineages derived from definitive LT-HSCs in the absence of FUBP1 at E15.5 are observed. Myeloid, erythroid and lymphocytic cells (B and T cells) are present to a comparable extent in wildtype (n=4) and *Fubp1*$^{null/null}$ (n=3) embryos. Data from 2 independent flow cytometry experiments are presented as the mean and SD; test for statistical significance: unpaired t-test.

Figure S2: FUBP1-deficient progenitor populations are able to differentiate into their respective mature hematopoietic lineages, related to Figure 1. Different progenitor populations (MEP, GMP, LMPP and MMP2) were isolated from E15.5 *Fubp1* GT1 +/+ (n=4) and *null/null* (FUBP1-deficient, n=3) fetal livers via FACS and evaluated for their colony formation potential. (A) FACS gating strategy used for progenitor sorting and representative FACS plots. (B) Number of colonies per 100 seeded cells. (C) Lineage potential of the different progenitor cells. Data are represented as the mean and were obtained in 2 independent experiments. Test for statistical significance: unpaired t-test.

Figure S3: Loss of LT-HSCs upon competitive transplantation of *Fubp1*$^{null/null}$ cells, related to Figure 2. (A) Representative flow cytometry plots of BM HSPC analyses 11 and 21 weeks after transplantation. The plots refer to the transplantation data of E15.5 fetal liver cells presented in **Fig. 2** of the manuscript.

Figure S4 (related to Figure 4): (A) Representative flow cytometry plots for the BrdU/7AAD cell cycle analysis of *ex vivo* cultured LT-HSC that were transduced with scrambled or *Fubp1* shRNA. The plots refer to **Fig. 4C** of the manuscript and demonstrate the decreased proliferative capacity of FUBP1-deficient LT-HSCs. (B) Working model of FUBP1 transcriptional regulator function in LT-HSC self-renewal. (C) *Fubp1* mRNA expression levels in different hematopoietic cell populations. Relative *Fubp1* expression was quantified via qPCR and normalized to the geometric mean of *Gapdh* and β*-Act* expression in FACS-isolated hematopoietic lineages. Data are presented as fold change over *Fubp1* expression in LT-HSCs and the mean and standard deviation of 3-4 independent experiments. Test for statistical significance: One-way ANOVA.

Supplemental Tables

Table S1: List of antibodies used for experiments, related to Figure 1.

Antibody/Substance	Clone	Company
CD11b AF647	M1/70	Biolegend
CD11b AF700	M1/70	Biolegend
CD11b BV421	M1/70	Biolegend
CD11b PE	M1/70	eBioscience
CD11b-Biotin	M1/70	eBioscience
CD135 PE	A2F10.1	BD Biosciences
CD150 BV605	TC15-12F12.2	Bioegend
CD150 PE	TC15-12F12.2	Biolegend
CD150 PerCP-Cy5.5	TC15-12F12.2	Biolegend
CD16/32 V450	2.4G2	BD Biosciences
CD19-Biotin	eBio1D3 (1D3)	eBioscience
CD34 AF647	RAM34	eBioscience
CD34 eF660	RAM34	eBioscience
CD3-BV510	17A2	Biolegend
CD3e-Biotin	145-2C11	eBioscience
CD3-V500	500A2	Biolegend
CD41-Biotin	eBioMWReg30 (MWReg30)	eBioscience
CD45.1 eF450	A20	eBioscience
CD45.2 APC	104	eBioscience
CD45.2 PerCP-Cy5.5	104	Biolegend
CD45R AF647	RA3-6B2	Biolegend
CD45R FITC	RA3-6B2	Biolegend
CD45R-Biotin	RA3-6B2	eBioscience
CD48 AF647	HM48.1	Biolegend
CD48 FITC	HM48.1	Biolegend
CD71 PE	RI7217	Biolegend
c-Kit PE-Cy7	2B8	eBioscience
Gr1 PE	RB6-8C5	eBioscience
Gr1-Biotin	RB6-8C5	eBioscience
Sca-1 Pacific Blue	D7	eBioscience
Sca-1 PerCP-Cy5.5	D7	eBioscience
Streptavidin APC-eF780	-	eBioscience
Ter119 AF647	TER-119	Biolegend
Ter119-Biotin	TER-119	eBioscience
Viability Dye eFluor® 506	-	eBioscience
Viability Dye eFluor® 780	-	eBioscience

Table S2: List of *TaqMan* assays used for qPCR-based gene expression analysis, related to Figure 4.

Gene Symbol	Assay ID
B2m	Mm00437762_m1*
Bcl2l1 (Bcl-X_L)	Mm00437783_m1
Bcl2l13 (Mil1)	Mm00463355_m1
CcnB1 (Cyclin B1)	Mm03053893_gH
Ccnd1 (Cyclin D1)	Mm00432359_m1
Ccnd2 (Cyclin D2)	Mm00438070_m1
Cdc42	Mm00846882_s1
Cdk4	Mm00726334_s1
Cdkn1a (p21)	Mm04205640_g1
Cdkn1b (p27)	Mm00438168_m1
Cdkn1c (p57)	Mm01272135_g1
Cdkn2d (p19)	Mm00486943_m1
c-Kit	Mm00445212_m1
c-Myc	Mm00487804_m1
Fubp1	Mm01311417_m1
Fubp3	Mm01328093_m1
Gapdh	Mm99999915_g1
Gata2	Mm00492301_m1
Gusb	Mm01197698_m1
HoxA10	Mm00433966_m1
HoxA5	Mm04213381_s1
HoxA9	Mm00439364_m1
HoxB4	Mm00657964_m1
Hprt	Mm00446968_m1
Khsrp (Fubp2)	Mm01232838_g1
Mecom ((Mds1-) Evi1)	Mm00514820_m1
Mecom (Mds1)	Mm00491303_m1
Meis1	Mm00487664_m1
Mpl	Mm00440310_m1
Nkap	Mm00482418_m1
Pmaip1 (Noxa)	Mm00451763_m1
Puf60 (Fir)	Mm00505017_m1
Pum1	Mm01180596_m1
Rac1	Mm01201653_mH
Rac2	Mm00485472_m1
Runx1	Mm01213405_m1
Sh2B3 (Lnk1)	Mm01196721_g1
Tal1	Mm01187033_m1
Vps72	Mm00656969_g1
β-Act	Mm00607939_s1

Supplemental Movie Legends

Movie S1: Long-term observation of murine wildtype LT-HSCs lentivirally transduced with *scrambled* control shRNA, related to Figure 4. Murine LT-HSCs and all subsequent progeny were observed to the 5th generation using time-lapse microscopy and cell tracking (tracks are shown as yellow circles). The observation time span was 3 h after LT-HSC sorting until 5 days, 23 h and 28 min of culture in serum-free medium supplemented with SCF and TPO. Phase contrast images are displayed in the left column; every 6th image frame was used to assemble the video (original temporal resolution: 2:30 min per frame). Successfully transduced cells were detected using nuclear Venus expression as indicated in the right panel. One fluorescence image was acquired each hour. All cells displayed normal generation times, and only one daughter cell underwent cell death during the observation time span. The time bar is displayed in day - h:min:sec. Movie S1 was assembled using QuickTime 7.7.3 software and corresponds to **Fig. 4D**.

Movie S2: Prolonged generation time and increased cell death rates in FUBP1-deficient murine LT-HSCs, related to Figure 4. Murine LT-HSCs and all subsequent progeny were observed to the 3rd generation using time-lapse microscopy and cell tracking until all cells were dead (tracks are shown as yellow circles). Observation of the cells started 3 h after LT-HSC sorting and ended at 7 days, 11 h and 47 min of culture in serum-free medium supplemented with SCF and TPO. Phase contrast images are displayed in the left column, and every 6th image frame was used to assemble the video (original temporal resolution: 2:30 min per frame). Successfully transduced cells were detected using nuclear Venus expression

as indicated in the right panel. One fluorescence image was acquired per hour. All daughter cells exhibited a prolonged generation time of more than 24 h and eventually died after one or two divisions. The time bar is displayed in day - h:min:sec. Movie S2 was assembled using QuickTime 7.7.3 software and corresponds to **Fig. 4D**.

Supplemental Experimental Procedures

Flow cytometric analysis of fetal erythroid and myeloid lineages. Embryo dissection and collection of embryonic blood was performed as previously described (Fraser et al., 2007) using E11.5 and E15.5 embryos. After drainage of the PB, FLs were isolated in PBS pH 7.4 containing 5% FBS. PB and FL cells were stained with antibodies against Ter119 (TER-117), CD71 (R17217), c-Kit (2B8), Mac-1 (M1/70), CD3 (17A2), B220 (RA3-6B2), and with Viability Dye eFluor® 780 (eBioscience) for discrimination of dead cells.

Progenitor colony formation assays. Wildtype or *Fubp1*$^{null/null}$ E15.5 FL cells were isolated, stained with biotinylated lineage antibodies against B220 (RA3-6B2), CD3 (145-2C11), CD19 (eBio1D3), Gr-1 (RB6-8C5) and Ter119 (TER-119) and fluorochrome-conjugated antibodies against Sca-1 (D7), CD117 (2B8), CD48 (HM48.1), CD150 (TC15-12F12.2), CD34 (RAM34), CD135 (A2F10.1) and CD16/32 (2.4G2). Streptavidin was added for detection of lineage$^+$ cells and Viability Dye eFluor® 506 was added for labeling dead cells. According to the sorting scheme in **Suppl. Fig. 2**, four different progenitor populations (MEPs (lin$^-$ c-Kit$^+$ Sca-1$^-$ CD16/32$^-$ CD150$^+$), GMPs (lin$^-$ c-Kit$^+$ Sca-1$^-$ CD16/32$^+$ CD34$^+$), LMMPs (lin$^-$ c-Kit$^+$ Sca-1$^+$ CD135$^+$ CD34$^+$; Mansson et al., 2007), and MPP2 (lin$^-$ c-Kit$^+$ Sca-1$^+$ CD135$^-$ CD34$^+$ CD150$^-$ CD48$^+$)) were sorted using a FACSAria III (*Becton Dickinson*). 300 MEPs and 100 GMPs/ LMPPs/MPP2 were seeded per ml M3434 medium (*Stem Cell Technologies*). For culturing MEPs the methylcellulose medium was supplemented with TPO (*Peprotech*) to a final concentration of 100 ng/ml. LMPP medium was supplemented with 50 ng/ml TPO and 50 ng/ml FLT3-L (*Peprotech*). MEP and GMP

colonies were microscopically scored at day 5 and LMPP and MPP2 colonies at day 7.

Western blot analysis. FUBP1 expression was detected via immunoblot using an anti-FUBP1 antibody (*Santa Cruz*, clone N-15) and a secondary rabbit anti-goat antibody (*Invitrogen*, cat.-no. 81-1620). As a loading control, β-actin levels were assessed using a rabbit-derived antibody (*Santa Cruz*, clone C-11) and a secondary donkey anti-rabbit antibody (*GE Health Care*, cat.-no. LNA934V).

Lentiviral *Fubp1* knockdown. Lentiviral shRNA expression constructs (*pLKO* vector-based) were obtained from *Sigma-Aldrich* (*Fubp1* shRNA #1: TRCN0000096803 and *Fubp1* shRNA #2: TRCN0000096801), and the puromycin resistance sequence was replaced by a Venus (nuclear membrane localized) fluorescence expression cassette. Infectious lentiviral particles were generated in HEK293T cells (DSMZ no. ACC 635) and then concentrated via ultracentrifugation as previously described (Thalheimer et al., 2014). LT-HSCs and MPPs were transduced with an MOI of 100-300.

Comparative *Fubp1* mRNA expression analysis in different hematopoietic cell populations. BMCs isolated from femurs and tibiae of *C57BL/6J* mice were stained either for mature hematopoietic lineages (antibodies against CD117 (2B8), CD3 (17A2), Mac-1 (M1/70), B220 (RA3-6B2), Gr-1 (RB6-8C5), Ter119 (TER-119), CD16/32 (2.4G2), Viability Dye eFluor® 780 (eBioscience)) or hematopoietic progenitors (biotinylated lineage antibodies against B220 (RA3-6B2), CD3 (145-2C11), CD19 (eBio1D3), CD41 (eBioMWReg30), Gr-1 (RB6-8C5), Mac-1 (M1/70) and Ter119 (TER-119), Streptavidin against the biotin conjugates, and antibodies

against CD117 (2B8), Sca-1 (D7), CD150 (TC15-12F12.2), CD48 (HM48.1), CD34 (RAM34), CD135 (A2F10.1), CD16/32 (2.4G2). The different hematopoietic lineages were directly sorted using a FACSAria I (*Becton Dickinson*) into the lysis buffer provided with the TaqMan PreAmp Cells-to-C_T Kit (*Ambion, Life Technologies*), which was also used for reverse transcription, pre-amplification and qPCR (LightCycler 480 System II; *Roche*) according to the manufacturer's protocol.

References:

Fraser, S.T., Isern, J., and Baron, M.H. (2007). Maturation and enucleation of primitive erythroblasts during mouse embryogenesis is accompanied by changes in cell-surface antigen expression. Blood *109*, 343-352.

Mansson, R., Hultquist, A., Luc, S., Yang, L., Anderson, K., Kharazi, S., Al-Hashmi, S., Liuba, K., Thoren, L., Adolfsson, J.*, et al.* (2007). Molecular evidence for hierarchical transcriptional lineage priming in fetal and adult stem cells and multipotent progenitors. Immunity *26*, 407-419.

Thalheimer, F.B., Wingert, S., De Giacomo, P., Haetscher, N., Rehage, M., Brill, B., Theis, F.J., Hennighausen, L., Schroeder, T., and Rieger, M.A. (2014). Cytokine-Regulated GADD45G Induces Differentiation and Lineage Selection in Hematopoietic Stem Cells. Stem cell reports *3*, 34-43.